Journal of Rock Mechanics and Geotechnical Engineering 14 (2022) 50–66

Contents lists available at ScienceDirect

Journal of Rock Mechanics and Geotechnical Engineering

journal homepage: www.jrmge.cn

Full Length Article

Deformation-based support design for highly stressed ground with a focus on rockburst damage mitigation

P.K. Kaiser [a,b,*], A. Moss [c]

[a] Laurentian University, Sudbury, ON, P3E 2C6, Canada
[b] GeoK Inc. 680 Ramsey Lake Road, Sudbury, ON, P3E 6H5, Canada
[c] Sonal Mining Technology Inc., 2488 Shadbolt Lane, West Vancouver, BC, V7S 3J1, Canada

ARTICLE INFO

Article history:
Received 3 January 2021
Received in revised form
28 March 2021
Accepted 9 May 2021
Available online 11 August 2021

Keywords:
Deep mining
Deformation-based support design (DBSD)
Cost-effective support
Support consumption
Preventive support maintenance (PSM)

ABSTRACT

As mines go deeper, mine designs become more fragile and effective rock support becomes a strategic element for ground control to facilitate timely construction and cost-effective access for uninterrupted production. This article focuses on the design of integrated support systems for brittle ground when large displacements due to gradual bulking of stress-fractured rock or sudden violent bulking during rockbursts are induced by static and dynamic loading. It provides an overview of support design principles for a rational approach to ground control in deep mines when large deformations are anticipated near excavations. Such designs must not only account for load equilibrium but also for deformation compatibility. Most importantly, the design approach must account for the fact that the support's displacement capacity is being consumed as it is deformed after support installation. It is therefore necessary to design for the remnant support capacity, i.e. the capacity remaining when the support is needed. Furthermore, if the support capacity can be consumed, it can also be restored by means of preventive support maintenance (PSM). The PSM concept for cost-effective ground control is introduced and illustrated by quantitative and operational evidence. Contrary to other design approaches, the deformation-based support design (DBSD) approach provides the capacity of an integrated support system as a function of imposed displacements. Reduction in this support capacity due to mining-induced deformation renders excavations increasingly more vulnerable if located within the influence of active mining and seismic activity. Because deformation measurements are robust indicators of the decay in support capacity, scanning and other displacement monitoring technologies enable measurements to verify the DBSD approach, to assess the remnant safety margin of the deformed support, and to make operational support maintenance decisions.

1. Introduction

1.1. Background

As mines go deeper, underground excavations become more vulnerable to damage and mine designs become more fragile. Consequently, ground control and rock support increasingly dominate construction schedules and production performance. Efficient and effective support becomes a strategic element of asset management because mine infrastructure and extraction developments are significant investments, particularly in caving operations. This investment must be protected and maintained to reduce the risk of ground related production disruptions (Moss and Kaiser, 2021). Furthermore, mining companies working at great depth, typically at depths exceeding 1500 m, have identified seismic hazards as a corporate risk and view ground control with reliable cost-effective support systems as a strategic tool in asset management.

In highly stressed ground, the support must not only be designed for load equilibrium but also for deformation compatibility. For this purpose, this article presents an innovative deformation-based support design (DBSD) approach for brittle ground when displacements induced by stress-fracturing after support installation consume much of the support's capacity. In such situations, it is necessary to design for the remnant support

* Corresponding author. Laurentian University, Sudbury, ON, P3E 2C6, Canada.
E-mail address: pkgeok@gmail.com (P.K. Kaiser).

Peer review under responsibility of Institute of Rock and Soil Mechanics, Chinese Academy of Sciences.

https://doi.org/10.1016/j.jrmge.2021.05.007

capacity, i.e. the capacity remaining when the support is needed. It is to be designed for the critical stage of its utility, not for the condition at the time of installation. This design aspect is not accounted for in standard rock classification systems used for support design and has often led to unnecessary excavation damage and production interruptions with economic consequences.

An underlying principle of the DBSD approach is that if support capacity can be consumed, it can also be restored by various means of proactive or preventive support maintenance (PSM). The rock support needs to provide a safe work environment and maintain an operationally functional excavation throughout its design life. In particular, the support has to eliminate or at least reduce the frequency of disruptive excavation damage. From a technical perspective, this means that the reinforced rock mass should remain self-supporting by creating deformable arches or wall panels, called 'gabion panels', that can adjust to large mining-induced deformation demands whether inflicted by static or dynamic loading (Moss and Kaiser, 2021).

1.2. Common practice

Common support design practices include:

(1) Empirical methods or rock mass classification systems such as Terzaghi's (1946) rock load classes and rock mass quality classes (rock mass rating (RMR) or modified rock quality index (Q')). These methods are applicable to conditions represented by the underlying data and tunnelling methods. As elaborated in this article, they are deficient when mining induces large displacements after support installation.
(2) Designs focusing on force equilibrium with defined failure mechanisms such as wedge instability (e.g. using tools like UNWEDGE™) and static or dynamic rock load models (e.g. paraboloid loading at intersections). They can be applied to shakedown analyses as introduced in Chapter 8 in Kaiser et al. (1996).
(3) Methods considering rock-support interaction using ground reaction curves for yielding ground to establish the equilibrium point between deformation-dependent load demand and support capacity, or by application of numerical models to simulate the loading of the support as the rock is deformed. This approach depends on the selected constitutive models representing rock, support, and their interaction. These approaches are only valid if the actual stress path is followed, i.e. when the simulated displacements are representative of the mining and support installation sequence. Unfortunately, rock mass strains and support loads are frequently underestimated by numerical models, particularly in brittle failing ground.
(4) Energy-centric design of rockburst support focusing on achieving equilibrium between dynamic energy demand and the ability of the support to dissipate energy. In this approach, the energy demand is typically compared with the capacity of an installed support rather than the capacity remaining at the time of a rockburst. This deficiency can be overcome by following the DBSD approach presented in this article.

Common practices and recent developments in ground support selection and design have been summarised by Potvin and Hadjigeorgiou (2020) with a special focus on support design for burstprone conditions in Chapter 13 and for risk-based approaches to ground support design in Chapter 16.

1.3. Best practice for support design

Common practices are not necessarily best practices when judged from an economic or workplace safety perspective (Kaiser, 2019). As in other engineering disciplines, it is necessary to systematically and continuously improve engineering design practices. Common practices that worked well at shallow depth may have to be replaced if the rock mass behaviour changes and poses new hazards, e.g. when mining at depth and working in highly stressed ground. Deficiencies of the common practices listed in Section 1.2 can mostly be attributed to mining-induced deformations consuming support capacity (particularly in Practices (1), (2), and (4) of Section 1.2). The actual deformation path that the rock mass experiences is rarely tracked by the support design process, and this creates a need to move from common to best practices by accounting for deformation-induced support system capacity (SSC) consumption.

1.3.1. Guiding principles of deformation-based support design

When support is installed near the advancing face, it is being deformed when the tunnel advances, when nearby excavations are opened, or when mining fronts progress over a supported drift. It is evident from Fig. 1 that the available support capacity is substantially less than that during support installation due to the wall displacements (which were more than 150 mm for these examples).

The design must respect that, at any point of the support's life, the remnant support capacity is less than the installed capacity. In other words, the actual factor of safety (*FS*) is gradually lowered by displacements imposed by mining and seismicity. Excavations become less safe with time due to the displacement-related support capacity decay. From a safety assessment perspective, it is not of interest what the capacity of the support is at the time of installation. Instead, it is necessary to establish the current *FS* and to maintain sufficient capacity when needed. In yielding and brittle fractured grounds, the design therefore must account for deformation-based support capacity consumption. This is consistent with geotechnical asset management approaches when designing open pits, tailings dams, landslide remediation, etc. (Dick et al., 2020).

1.3.2. Deformable support design approach

The workflow for support design consists of four elements (Fig. 2):

(1) Identification of the vulnerability of excavations to all possible failure modes;
(2) Establishment of engineering design assumptions and parameters and selection of suitable support systems;
(3) Design analyses to estimate the demands imposed on the support and the support system capacities, and to obtain the safety margin (or *FS*) over the life of an excavation;
(4) Verification of the reliability, robustness, and limitations of the design and specification of support maintenance requirements over the design life.

For this purpose, the ground control engineer has to:

(1) Identify excavations that are vulnerable to damage and establish the dominant excavation behaviour;
(2) Define (and register) design assumptions and dominant design parameters (including their variability) as well as applicable rules or models such that a suitable support system (class) can be selected;

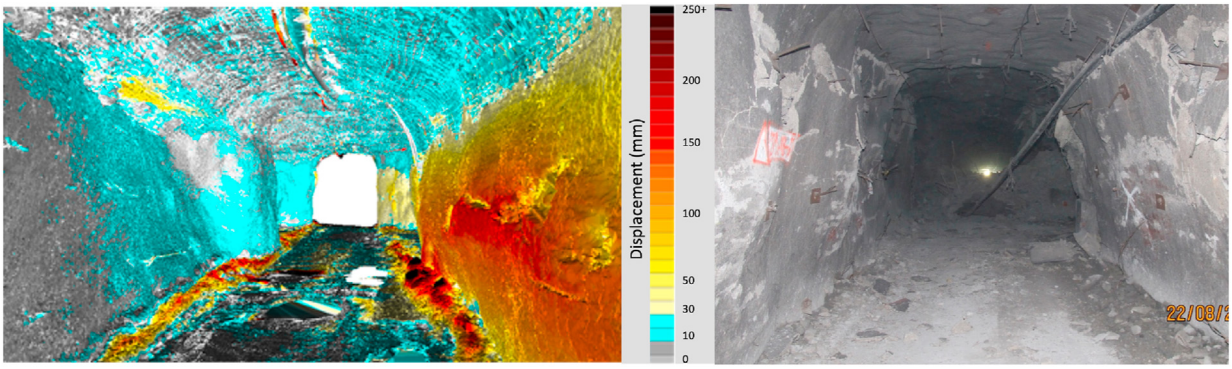

Fig. 1. (a) Digital displacement survey results of tunnel damaged by strainburst behind the supported wall on the right, and (b) photo illustrating the damage experienced by a support system with threadbar and plain cable bolts when deformed by rock mass bulking behind the areal support (AS) consisting of mesh-reinforced shotcrete (Courtesy: PT Freeport Indonesia).

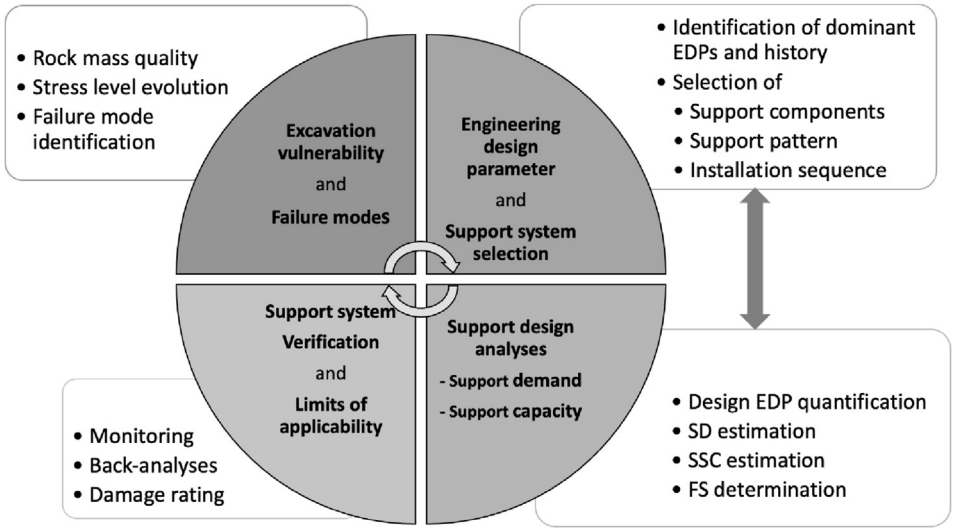

Fig. 2. Workflow for underground support design. EDP - engineering design parameter; SD - support demand.

(3) Undertake design analyses with applicable empirical or semi-empirical design rules (e.g. span to bolt length rules) and appropriate models to establish the demands and the capacities of the support systems, and obtain the safety margin (or *FS*);
(4) Modify the design, if necessary, verify the reliability and robustness of the design, and specify the limits of applicability (revise assumptions if necessary); and
(5) Specify a PSM (capacity restoration) plan to account for mining-induced support consumption over the design life.

In the following sections, the design analyses utilizing the DBSD approach are presented together with technical justifications.

1.3.3. DBSD for burst-prone ground

Independent of rockburst type (fault slip, pillar burst or strainburst), this support design methodology consists of five design components (see Fig. 3): (1) hazard assessment, (2) demand estimate (load, displacement and energy), (3) estimate of support component and support system capacities (load, displacement, and energy), (4) appropriate support systems selection by matching SSC with anticipated demand, and (5) design verification and modification through displacement monitoring.

Although the overall design approach consists of only five main components, the detailed steps involved in the design process are complex, requiring various iterations and comparisons of alternatives. Most importantly, the impact of the deformation history and the displacement and energy demands from static and dynamic rock mass failure processes have to be considered. The respective sources of demand are listed on the right of Fig. 3. They consist of displacement demands before a support system is loaded by a rockburst, and displacement and energy demands imposed by a rockburst. In the following, energy demands from strain energy stored in the failing rock and the surrounding rock mass are ignored, because much of this energy can be consumed during the fracture process and by friction and heat in effectively supported ground.

Specifically, the displacement demands should consider pre-event mining-induced displacements since support installation (represented later by a design parameter d_0), and the sudden bulking of the strainburst volume magnified by straining from distant or remote seismic events. The energy demands stem from the acceleration of the fractured rock in front of the strainburst volume (called 'burden') and part of the burst volume. This acceleration may be enhanced by the (peak) ground motion (PGV) from a distant seismic event. These demand components are explained in more detail in Section 2.3.

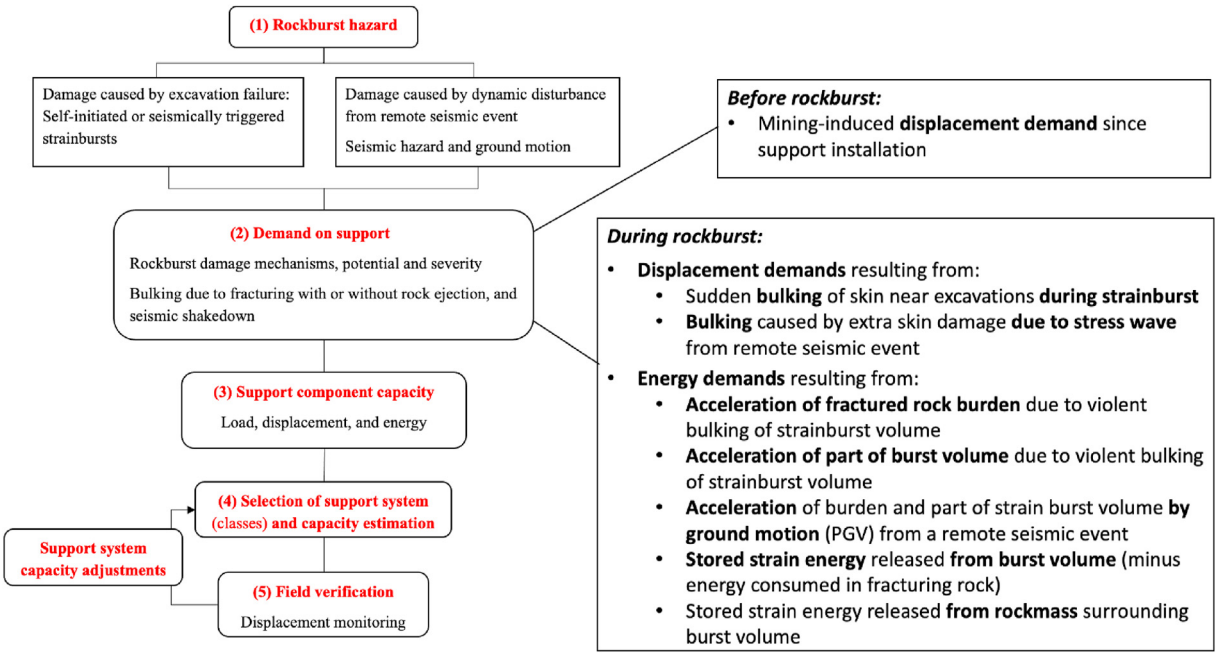

Fig. 3. Workflow for support selection in burst-prone ground (modified after Cai and Kaiser, 2018). PGV stands for peak ground velocity.

1.3.4. Observational design verification and optimisation

Life-cycle design and maintenance of civil and mining structures are moving to performance-based engineering whereby innovative engineering solutions are found by integrating performance monitoring into the design process. For example, in slope or open pit engineering, displacement monitoring by radar or LiDAR is a standard practice for design verification and operational decision-making. These advances have revolutionized slope design by seamlessly integrating displacement data into the design and performance assessment process.

Emerging displacement monitoring for convergence and rock mass deformation monitoring in underground construction and mining therefore offer opportunities to utilize displacement monitoring for support design verification and optimisation, safety assessment, and preventive maintenance of infrastructure. Because design outputs must be congruent with those measured in the field (i.e. wall displacements), displacement monitoring offers a means to improve support design by adopting a DBSD approach for civil engineering tunnels in stressed ground, and for mining when large deformations are induced by static and dynamic mining-induced loading.

The motivation for the proposed move to the DBSD methodology is therefore partly driven by technology developments that allow for rapid and reliable measurements of mining-induced displacement responses of excavations and support systems. In this manner, the safety margin of a gradually deformed support system can be assessed, cost-effective support systems can be selected and designed, and PSM can be targeted and executed in a timely manner.

2. Excavation damage mechanisms and support demand

The design of any engineering structure involves an assessment of imposed demands relative to the available capacities to resist the demands, i.e. $FS = capacity/demand$. In underground excavations, the load, displacement or energy demands depend on the possible modes of instability.

2.1. Characterisation of excavation behaviour

The excavation behaviour can be characterised by nine modes as illustrated by the 3×3 excavation behaviour matrix (see Fig. 4). The horizontal axis represents the rock mass quality (RMQ quantified by the modified rock quality index Q' (with SRF and $J_w = 1$), the rock mass rating (RMR), and the Geological Strength Index (GSI)) or the rock mass strength, and the vertical axis represents the stress intensity or stress level (SL, represented by the stress level index, $SLI = \sigma_{max}/UCS = (3\sigma_1 - \sigma_3)/UCS$, where σ_1 and σ_3 are the principal far-field stresses at the location of the tunnel, UCS is the uniaxial compressive strength). With increasing stress, instability modes change from gravity-driven to stress-assisted, and to stress-driven failure modes. With decreasing rock quality, the failure process changes from brittle failure of massive or moderately jointed ground, to falls of ground or shake down failures, and to progressive unravelling and squeezing ground in weak and soft ground. In other words, excavations in massive to continuously jointed but interlocked ground are prone to stress-fracture and strainburst near the excavation (stars in Fig. 4); excavations in fractured or blocky ground to disintegrated rock are prone to failure with some structural controls; and excavations in highly fractured or sheared ground are prone to falls of ground, shakedown or unravelling processes and large plastic deformation.

In deep hard rock mines, a strainburst involving sudden and violent failures of rock is caused by excessive strain of a volume of stiff and strong rock (called 'burst volume') near an excavation boundary. For self-initiated or mining-induced strainburst, the primary seismic source is co-located with the damage location. For triggered strainburst, the damage is initiated by stress waves from a distant seismic event, and the secondary seismic source is co-located with the damage location.

A dynamically loaded strainburst is a strainburst that is augmented by the impact of energy radiated from a primary source in two possible forms:

(1) The radiating energy causes a sequence of dynamic stress pulses that may deepen the depth of failure and release more

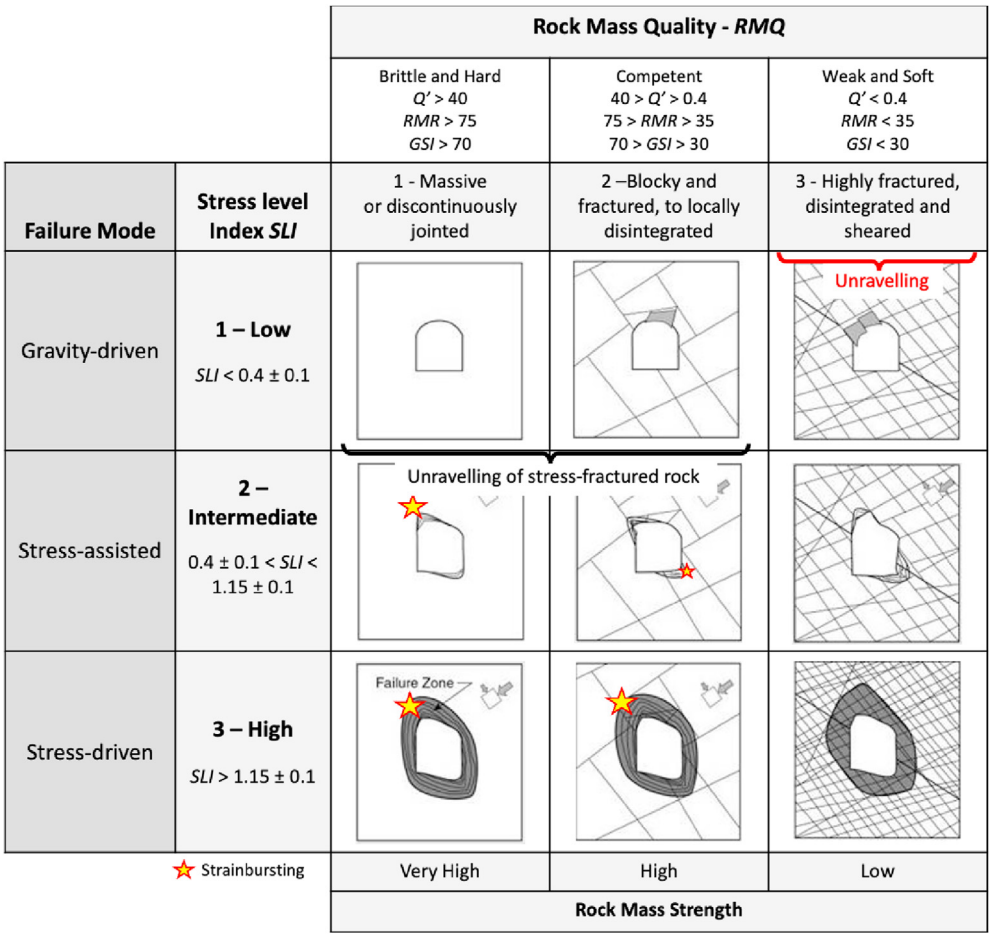

Fig. 4. Excavation (drift or tunnel) behaviour matrix (modified after Kaiser et al. (2000) and Kaiser (2019)).

stored strain energy through rock mass bulking imposing additional strains or displacements to the rock and support; and

(2) The distant seismic event may transfer some of its radiated energy to kinetic energy and eject part of marginally stable rock.

For dynamically loaded strainburst, the secondary seismic source is also co-located with the damage location.

A strainburst may also occur inside a well-supported rock mass, i.e. behind the AS consisting of mesh or shotcrete, in the reinforced rock, or behind the supported ground. Such a restrained strainburst may cause internal damage to the support system and may lead to the ejection of rock and support components.

2.2. Vulnerability and fragility

The vulnerability of an excavation is a measure of the possibility of being exposed to physical damage. Strictly speaking, it is the probability of damage occurring due to a specific threat, without consideration of the severity of the resulting damage. The fragility is the quality of being easily broken (antonym: robustness). It is the probability of an undesired outcome (exceeding a given damage level or production consequence) of an excitation. For example, highly vulnerable excavations are more likely to be damaged, but robust excavations will suffer less damage than fragile ones under the same seismic event intensity.

2.2.1. Vulnerability

Vulnerable excavations may therefore fail by falls of ground, rock mass yield or bulking of stress-fractured rock, strainbursting with or without rock ejection, and rock ejection resulting from the energy transfer from a distant seismic source. A summary of the historical development of the concept of excavation vulnerability was presented by Kaiser (2017a) together with a detailed discussion of the vulnerability of excavations in burst-prone ground.

During the support selection process, the vulnerability for each potential failure mode (see Fig. 4) and the sensitivity to various factors must be assessed. For static loading, rock mass bulking causing large static deformations near excavations during stress fracturing is dominated by the depth of failure and the mining-induced tangential strain in the excavation wall, and for dynamic loading:

(1) Shakedown is dominated by rock quality, span, and the acceleration from dynamic disturbances;
(2) Strainbursting with or without rock ejection is dominated by the stored strain energy and the loading system stiffness and in situ stress field;
(3) Rock mass bulking causing large static and dynamic deformation near excavation during stress fracturing is dominated by the depth of failure, mining-induced tangential strain in the excavation wall, and the stress wave from distant seismic events; and

(4) Rock ejection by energy and momentum transfers from a distant seismic source is dominated by the energy transmitted from the seismic source (considering radiation patterns).

If an excavation is vulnerable, dynamic disturbances can bring it to the point of failure, called 'trigger point'. Once failure is initiated, the excavation damage process will continue until a 'new' equilibrium is established when the energy inputs from various sources (ground motion, stress release, and rock mass deformation) are consumed by energy sinks (rock fracturing and rock mass deformation including the installed rock support). If a 'new' equilibrium can be reached, the failure process is arrested, and collapse of the excavation is prevented. This is called the 'survival state' (Kaiser et al., 1996). If not, some rock and parts of support components will be ejected, and the excavation will be damaged.

2.2.2. Fragility

For underground excavations, the fragility defines the likelihood of an undesired outcome (a given damage level R) of three excitations: load, displacement, or energy demands imposed on the excavation. The higher a demand, the higher the likelihood for damage with higher damage ratings R (e.g. Heal et al., 2006). Effectively supported excavations will suffer less damage than fragile ones with insufficient support. Severe damage is less likely to occur for robust and effective support systems. A primary goal of DBSD therefore is to provide robust support systems that are less likely to be severely damaged.

2.2.3. Implications for support design

Because severe damage is more disruptive to mine operations (Moss and Kaiser, 2021), a robust support system should be effective at high demand levels after large displacements are imposed. Hence, the goal of DBSD is not just to achieve a desired *FS* at the time of installation, but to reduce the fragility of an excavation by preventing highly disruptive and severe damage (R4 or R5; see Appendix A).

This leads to a fundamental shift in support design. The support is to be designed such that it performs well when it is deformed, i.e. after some of its capacity has been consumed. The reason why severe and highly disruptive damage is observed can often be attributed to the fact that the safety margin of the support has been lost prior to a rockburst event. In highly deformed ground, the actual *FS* when the support is needed is much lower than the 'installed' *FS*. In other words, the support is to be designed for an operationally acceptable state.

This leads to two practical alternatives:

(1) Design the support for a high pre-event *FS*, such that the consequences of displacement demand can be covered; or
(2) Adopt a PSM program to strategically maintain the 'installed' *FS* by adding supplemental support capacity where needed.

Whereas it is common practice to aim at single pass support systems, in highly deformed ground, this is rarely cost-effective because of high variability in mining-induced displacement demands. As will be discussed later, PSM aims at reducing the fragility of excavations once some damage (R0 to R3; see Appendix A) has been observed, and by restoring some of the lost capacity at strategic locations such that the support remains robust enough for future demands. As discussed by Moss and Kaiser (2021), the cost and related delays of PSM is far less than those by severe excavation damage. Furthermore, the cumulative cost of single pass systems with sufficient margins to survive at large displacements can also be far more expensive than when the support is designed for PSM following DBSD principles. The rating tables in Appendix A provide guidance on assessing the feasibility of PSM for conditions when excavations are exposed to dynamic loading from rockbursts and are prone to various levels of damage.

2.3. Support demands

Depending on the failure mode, different static load and displacement demands are imposed on the support. When combined with dynamic loading, the gravitational load is increased by dynamic acceleration, and the displacement demand is increased by dynamic displacement increments (co-seismic straining). Energy is imposed by ground motion resulting from seismic waves and the sudden bulking displacements by the stress-fractured rock during a strainburst. This article mainly focuses on the displacement and energy demands in brittle failing rock.

2.3.1. Load demand

The bolt load demand is typically defined as mg and $m(g+a)$ for static and dynamic loadings, respectively, where m is the mass of supported rock and g the gravitational acceleration (Chapter 8 in Kaiser et al., 1996). This applies to wedge- or paraboloid-like unstable rock volumes at the back of excavations. The load is transferred to the bolts via the mesh, plate, and anchor sections of the bolts. Because the load capacity of the support system must be higher than the load demand to prevent failure, the resulting static bolt displacement must be less than the displacement needed to reach the maximum load of at least one of the bolt types that makes up the support system.

Under dynamic loading by stress waves passing an excavation, the load may temporarily exceed the yield capacity if the energy demand can be dissipated by work done by the support system before the ultimate displacement capacity of the support system is reached (i.e. survival of the dynamic loading; see Section 3.1). The approach proposed in Chapter 8 by Kaiser et al. (1996) is suitable to assess the shakedown hazard as a function of a support system's ductility or ultimate displacement capacity.

2.3.2. Displacement demand

The displacement demand consists of a static or gradual displacement imposed after support installation, and a dynamic displacement increment imposed by the bursting ground.

(1) Static displacement

The static displacement demand is typically obtained by analytical (ground reaction curve) or numerical models considering elastic and plastic deformations. In brittle failing rock, the static displacement can be obtained by estimating the depth of failure d_f and the bulking of the fractured rock described by a linear bulking factor (BF) (Kaiser, 2016).

(2) Dynamic displacement resulting from strainburst

When impacted by a stress wave from a distant seismic event, a strainburst of depth d_{SB} may be triggered (Gao et al., 2019a, b). The depth of static failure increases by an increment $\Delta d_f = d_{SB}$, and the bulking factor by an increment ΔBF due to the shaking motion. Therefore, a dynamic displacement increment is imposed on the support. The static and dynamic displacement demands are commonly ignored in conventional energy-centric support design approach, as it is assumed that an energy demand, i.e. related to

PGV^2 from a distant seismic event, is imposed via a mass of supported rock in the un-deformed support (on the 'installed' support).

As Fig. 5b illustrates, burst damage is often associated with large displacements that lead to bolt failure and bulging of the AS. This displacement is caused by the bulking of rock in a burst volume (Fig. 5a) when driven to failure by tangential forces (F) in stress raisers (red) near the excavation. Because of the tangential strain, broken rock is forced into the excavation and the resulting radial displacement δ (see Eq. (1)) is imposed on the support at the plate and to some extent by straining the bolts inside the rock mass.

$$\delta = d_{SB}\, BF \tag{1}$$

where BF ranges from as high as 30% for unsupported to 15% for lightly supported and to a few percent for well-reinforced and well-confined rock. For example, 1 m of bursting rock, bulking at $BF = 5\%$, imposes a displacement of $\delta_{SB} = 50$ mm at the inner edge of the burst volume (dashed red in Fig. 5c). If there is a burden of statically damaged rock d_f^0 in front of the burst volume, it is pushed into the excavation by δ_{SB}. The displacement demand from this strainburst is 50 mm at the inner edge of the strainburst volume and at the front of the burden (if it is incompressible). It is zero at the back of the strainburst volume. A rock bolt crossing the burst volume will experience an average strain equal to BF (5% in this example).

(3) Dynamic ground motion resulting from strainburst

The strainburst displacement δ_{SB} is imposed on the support independent of the ground motion caused by the distant seismic event. The corresponding velocity of the inner edge of the burst volume v_i (see Fig. 5c) depends on the time required to bulk the burst volume. This time is called the 'rupture time' (t_R) of the strainburst volume (or the event duration, i.e. the duration of the strainburst). Preliminary back-analyses of rock ejected by strainbursts in unsupported ground suggest that t_R ranges from 50 ms to 100 ms; in rare cases, $t_R = 20$ ms was obtained. Event duration times of 30–50 ms have been back-analysed for a number of strainburst by the Institute for Mine Seismology (IMS) for a limited number of rockburst events. The velocity v_i on the inside of the burst volume can therefore be estimated by $v_i = \delta_{SB}/t_R$. For this example with $t_R = 50$ ms and $\delta_{SB} = 50$ mm, $v_i = 1$ m/s.

2.3.3. Energy demand

In burst-prone ground, energy demands come from two sources: the violent failure of the excavation due to excessive tangential strain of brittle failing rock inside the burst volume (Section 2.3.2), and energy transferred to potentially vulnerable ground from a distant seismic event (i.e. fault slip event or earthquake).

(1) Energy from strainburst (SB)

The strainburst displacement δ_{SB} is imposed on the support and is independent of the ground motion caused by a distant seismic event. The corresponding velocity of the inner edge of the burst volume is v_i.

If a burden (B) of thickness d_B and a mass m_B in front of the burst volume is moved at this velocity, its initial kinetic energy, before being decelerated by work done by the support system, is $E_{iB} = m_B v_i^2/2$. The burst volume will move at an average velocity $v_i/2$ (v_i at front and zero at back of burst volume), thus the maximum initial energy of the burst volume is $E_{iSB} = m_{SB} v_i^2/4$. If unsupported, the ejection velocity of the burden is v_i and the maximum energy of the total ejected mass is $E_{ej} = (m_B/2 + m_{SB}/4)v_i^2$, e.g. approximately 1.5 kJ/m^2 for $v_i = 1$ m/s with $d_{SB} = 1$ m and $d_B = 0.5$ m. In other words, a self-initiated or triggered strainburst without energy input from a distant seismic event (with $PGV \approx 0$) can eject 1.5 m^3 of rock at 1 m/s without momentum transfer effects. If some of the momentum of the burst volume or burden is transferred to smaller pieces of rock, the ejection velocity of these smaller pieces can be much higher (Stacey, 2016).

In addition, other sources of energy release may have to be considered. For example, displacements may be magnified by buckling motions or part of the stored strain energy may be released, particularly if the strainburst occurs in stiff rock (stiff dykes) embedded in a softer rock matrix. Some of the stored strain energy, however, is consumed as fracture energy, by friction and generation of heat. These extra sources of energy are not discussed in this article to focus on displacement-driven damage processes.

(2) Energy from distant seismic events

Large seismic events emit stress waves and transmit energy from the source to a potential strainburst location or to marginally

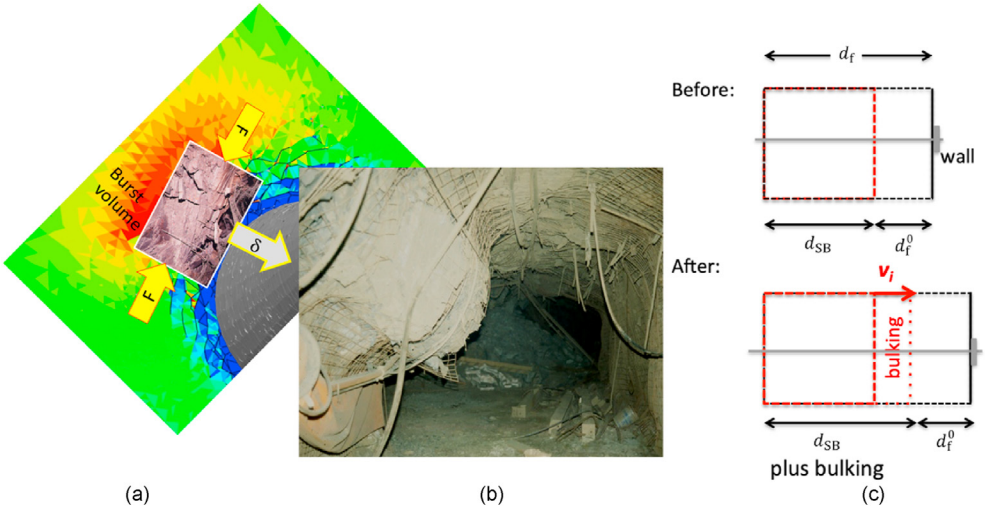

Fig. 5. (a) Maximum principal stress contours indicating location of elevated stress (red) and load on a 'burst volume', (b) Strainburst damage of light support with rebar and mesh, and (c) Geometric definitions for strainburst model.

stable blocks of rock near excavations. The dynamic stress wave temporarily increases and then decreases the tangential stress near the excavation, and this could deepen the depth of failure, increase the strainburst hazard, and create an unravelling hazard due to the temporary relaxation of clamping forces. The shaking motion may also increase the *BF* and the amount of wall deformation. Consequently, the extent of excavation damage would increase as a result of the action of large distant seismic events, leading to increments of displacement and initial velocity.

In addition, the ground motion from the distant seismic event may simultaneously accelerate the burden and burst volume, adding an energy increment of $\Delta E = (m_B + m_{SB})\,(nPGV)^2/2$, where n is a potential magnification factor (Kaiser et al., 1996; Stacey, 2016). For the above example, a distant seismic event with $PGV = 2$ m/s (anticipated for an event of magnitude $M_L = 3.3$ at a distance $R = 30$ m) would add 8.3 kJ/m^2 (for a combined 9.8 kJ/m^2 if acting simultaneously with the strainburst energy, see Section 2.3.3).

Field evidence collected by Morissette et al. (2012) suggests that the demand generated by the strainburst dominates for seismic events of low magnitude (i.e. $M \leq 2$; Kaiser, 2017b). For larger seismic events (M>2), the energy demand is increasingly augmented by the energy transmitted from the distant seismic event.

2.3.4. Demand path in displacement–energy space

The combined effects of the displacement and energy demand are illustrated by the demand paths shown in Fig. 6 for conditions similar to those presented in the example (Section 2.3.3). Two scenarios are shown: (i) for ejection of burden alone (black line with circles), i.e. the burst volume only bulks but is not ejected, and (ii) for ejection of the burden and strainburst volume (red line and triangles). Each load path involves three displacement increments (1–3) and two energy increments (2 and 3) as explained in the caption. The dashed curve presents an approximation of the demand path by a nth-order hyperbolic loading path for an ejection of the burden plus half the strainburst volume. This approximation is used in Section 3 to compare the demand with the SSC.

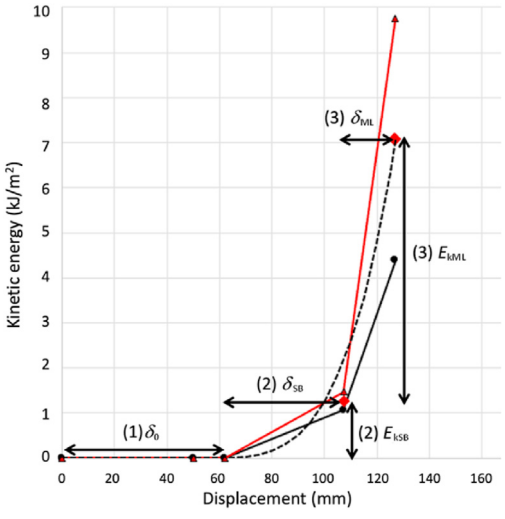

Fig. 6. Displacement–energy path for an example with similar conditions as described in the text (red line with triangle): (1) $\delta_0 = 61$ mm of initial, mining induced displacement (including bulking of burden) before impact by dynamically loaded strainburst, (2) 47 mm of strainburst bulking and 1.3 kJ/m^2 energy release, and (3) 20 mm of bulking due to stress wave impact and 5.8 kJ/m^2 energy transfer for $PGV = 2$ m/s.

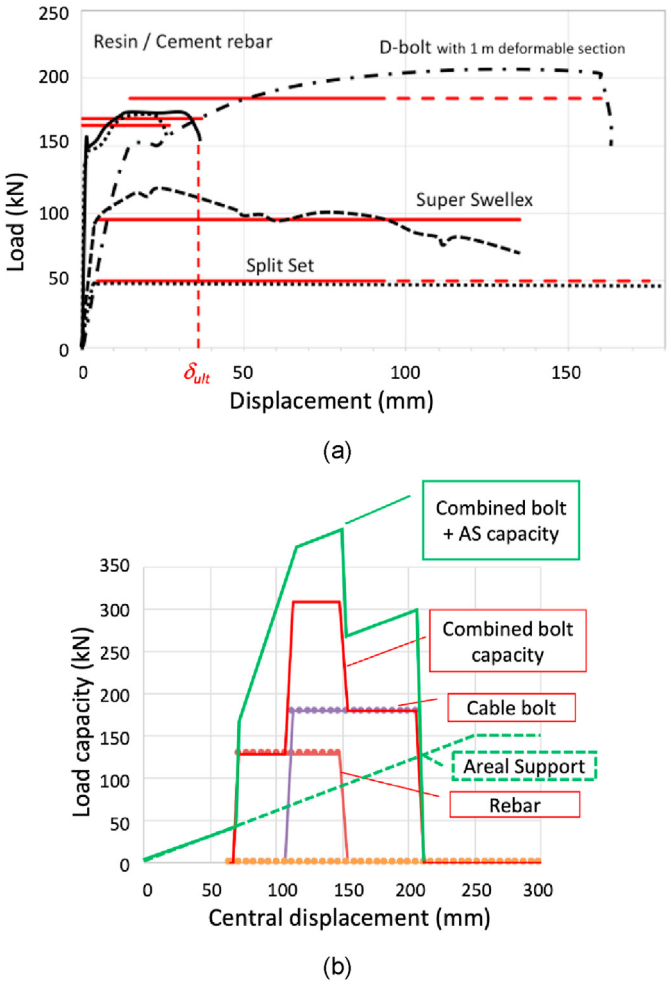

Fig. 7. (a) Load–displacement characteristics of individual bolts with perfectly plastic approximations in red, and (b) Combined load capacity of integrated support system (full green) consisting of an AS (green dashed) and two bolt types (rebar and cable bolt at regular bolt spacing). Note that the central displacement is the displacement between the bolts, consisting of the bolt head plus the AS deflection.

Fig. 6 illustrates the demand path for a situation where static mining-induced displacements including bulking of the burden impose a pre-burst displacement $\delta_0 = 61$ mm on the support. A strainburst primarily deforms the support (adding $\delta_{SB} = 47$ mm) with a relatively small energy release ($E_{kSB} = 1.1$–1.5 kJ/m^2 for burden only and with full strainburst volume). The impact of a distant seismic event with $PGV = 2$ m/s adds comparatively little bulking displacement, $\delta_{ML} = 20$ mm, but more energy ($\Delta E_{kML} = 3.3$–8.3 kJ/m^2 for burden only and with full strainburst volume; for a total of $E_{kSB\,+\,ML} = 4.4$–9.8 kJ/m^2). The ultimate displacement demand for ejection of burden plus half of strainburst volume is 61 + 47 + 20 = 127 mm and 7.1 kJ/m^2 (red diamond).

It follows that the strainburst process imposes much displacement on the support before the energy demand loads the support. The consequences of the hyperbolic loading path on the support behaviour is discussed in Section 3.2.3.

2.3.5. Implication for support design

The demand path in Fig. 6 is not vertical (starting at $d_0 = 61$ mm and $E = 0$ kJ/m^2) as commonly implied in energy-centric support design approaches. The support is pre-deformed by static mining-induced displacements and then deformed by bulking displacements as it is gradually impacted by the energy demand. As

demonstrated in Section 3.2.3, this means that some of the support's 'installed' energy capacity has already been consumed when it experiences the energy demand imposed by a rockburst.

3. Estimation of SSC

A support system is made up of various support components, i.e. bolts or cables for reinforcement and to provide a holding function, and AS to retain broken rock between bolts. The capacity of each component is a function of the imposed displacement as illustrated by the examples in Fig. 7a, reaching the yield strength F_y at δ_y and the ultimate capacity F_{ult} at d_{ult}. For simplicity, the load–displacement characteristics of the bolts are approximated by a perfectly plastic model (red in Fig. 7a) with a constant mean bolt load F_m. The actual characteristic can be followed in more refined models. The work done by the bolt at failure, W_{ult}, is equal to the area under the load displacement curve, i.e. $W_{ult} = F_m d_{ult}$. For AS, it is approximated by a triangular load–displacement characteristic (dashed green in Fig. 7b) such that $W_{ASult} = F_{ASult} d_{ult}/2$. For burst-resistant rock support design, the dynamic load–displacement characteristics can be approximated in the same manner.

3.1. Displacement-dependent load capacity

Individual support components are activated by the imposed mining-induced displacement, e.g. the displacement transferred from the rock via the grout to a rebar or cable bolt. It is reasonable to assume that radially installed bolts get simultaneously strained. However, they may be activated at different initial displacements d_i. For the case presented in Fig. 7b, the AS is loaded immediately, followed by the rebar and cable. As a consequence, the SSC evolves with increasing displacement and depends on the installation sequence if displacements occur between bolt activation stages. For the simplified load–displacement model, the SSC is stepped as shown in Fig. 7b (red for the bolts and green for the support system including the load carried by the AS). In this example, the AS is assumed to deform by 60 mm and 110 mm before the rebar and the cable bolts are activated, respectively. In this scenario, it is assumed that the AS is robust enough to retain broken rock until both bolt types fail.

If the static load demand is less than 130 kN in this case, the AS will deform (bulge between bolts) to 60 mm and the rebar will remain in the elastic deformation range. The cable bolts will not be activated until the load exceeds the rebar's capacity and 30 mm of yield deformation occurs in the rebar before the movement gets arrested by the cable bolts. Both the rebar and cable bolts yield at a combined load of 305 kN. For example, at a load demand of 153 kN, the $FS_L = 2$ in terms of the combined bolt capacity, and 2.5 in terms of total load capacity of the integrated support system with bolts and AS.

At 150 mm, after the cable bolts' load capacity is reached and the rebar reaches its ultimate displacement capacity and fails, the support system's load capacity drops from 390 kN to 270 kN (by 31%) and then to zero at 205 mm when the cable bolts also fail.

In summary, whereas the numbers in the example depend on the assumed support component characteristics, the most important message from Fig. 7 is that the load capacity of a support system is not constant; it evolves as it is deformed. For this example, the *FS* decays after 150 mm of displacement and the support system eventually fails when all bolt types fail at 205 mm. Locally, this support system will be damaged long before the support system collapse, i.e. when the rebar fails and the effective bolt spacing increases to the spacing of the cable bolts (see Section 3.2.3).

3.2. Displacement-dependent energy capacity

3.2.1. Overall SSC

When support components are deformed, work is done by each support component and the consumed energy accumulates. Fig. 8 presents the load–displacement curve (plotted against bolt head displacement and normalised per m^2) of a support system consisting of debonded Posimix bolts and cable bolts of comparable load capacity and an AS system with an allowable displacement capacity of $d_{ult} = 250$ mm. In this example, the bolts are activated after $d_i = 25$ mm and 50 mm of displacements with $d_{ult} = 110$ mm and 40 mm, for the debonded Posimix and cable bolts in direct loading, respectively (d_i depends on the bolt installation sequence, mining-induced pre-deformation, and the seating deformation for each bolts type). Because of the ductility of the debonded Posimix bolts, the cable bolts fail first in this example. The deformation of the AS depends on its bending stiffness, i.e. low for mesh and straps, moderate for mesh-reinforced shotcrete, and high for multi-layer AS systems. For the models presented in this article, it is assumed that the AS deforms as much as the bolts (i.e. the total central deflection between the bolts is twice the bolt head displacement).

For this example, the support system will yield at a static load of 86 kN/m^2 and fail at 173 kN/m^2. If temporarily overloaded by 'seismic hammering' such that both bolt types yield, co-seismic displacements will accumulate, and the support system will lose 50% of its maximum capacity at 88 mm and eventually collapse at 134 mm of displacement.

The energy–displacement characteristics of this support system are obtained by superposition of work done by simultaneously deformed support components. After each component is activated, its remnant capacity decreases until it is used up at d_{ult} for each component ($d_{ult1\&2}$). This is illustrated in Fig. 9a for the adopted model with constant F_m and a constant work split ($m = 25\%$). This figure presents the remnant capacities of two bolt types (red dotted and dashed), activated at $d_{i1\&2}$, and an AS activated at zero displacement (green dashed). The combined remnant energy capacity shows a peak of 30 kJ/m^2 upon activation of the second bolt type (cable bolt). It increases each time when a bolt type gets

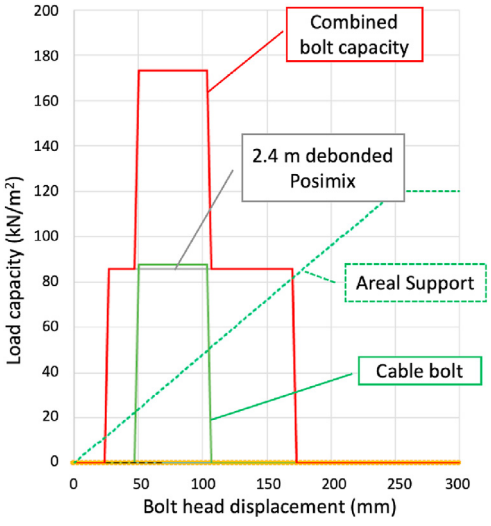

Fig. 8. Load–displacement characteristics of an SSC consisting of an AS (green dashed; mesh-reinforced shotcrete) and two bolt types (2.4 m debonded Posimix bolts and single cable bolts at 1.3 m spacing) for direct and indirect loading with work split parameter $m = 25\%$.

activated and then gradually drops until failure of the bolting system occurs at 130 mm of displacement.

The cumulative work done by the support system (AS plus bolts), which corresponds to the area under the combined load capacity curves (see Fig. 8), is shown in black (full line) in Fig. 9a and b. The ultimate capacity of this support system is 30 kJ/m^2 because the support system collapses when both bolt types fail at 130 mm (indicated by red ' × ' and vertical dashed line in yellow). This energy capacity is less than the arithmetic sum of the ultimate energy capacities of the individual components (36 kJ/m^2 at 250 mm as indicated by the black dashed line). In this example, the difference is relatively small (6 kJ/m^2 or 17%); however, depending on the installation sequence, the ultimate capacity of a support system can be much lower than the arithmetic sum of the ultimate energy capacities of the individual components.

The remnant energy capacity of the support system is shown in Fig. 9b (solid red line). It starts at 30 kJ/m^2 and gradually drops to zero at 130 mm of displacement. This line defines the available remnant energy capacity, as a function of the imposed displacement, i.e. the energy demand that the support could sustain if impacted at a given displacement. This support system has an energy capacity of 23 kJ/m^2 at 50 mm support system displacement once both bolt types have been installed and activated. If this support system with a theoretical cumulative capacity of 36 kJ/m^2 is gradually deformed, it has at best a capacity of 23 kJ/m^2 (64%) right after cable bolt activation, and less if deformed after cable bolt installation by rockburst loading or rock mass bulking. At 100 mm of displacement, for example, only 7 kJ/m^2 of energy capacity remains.

3.2.2. Implication for support design

Much of the support system's initial energy capacity can be consumed by mining-induced static or co-seismic deformations. The theoretical cumulative capacity is never available to mitigate rockburst damage. By the time all support components are installed, the energy capacity is significantly reduced (to 64% for the example in Section 3.2.1). When the first component in the support system fails (at 100 mm for the example in Section 3.2.1), the remnant SSC (18% for the example in Section 3.2.1) may be insufficient to resist imposed displacement and energy demands from a rockburst. This example clearly underlines the need for DBSD. Without consideration of the displacement history, the available SSC will be overestimated.

3.2.3. Local SSC (LSSC)

The SSC assessment presented in the previous section is applicable when the entire support system is deformed by external loading until all bolts reach their respective ultimate displacement capacities (d_{ult}). Fig. 9 describes the remnant capacity of the entire support system (called 'overall SSC').

If the loading process is purely driven by displacements, the aforementioned overall SSC can be reached. However, if a support system needs to do work to dissipate energy during dynamic loading, the load path in the d–E space (e.g. Fig. 6) reaches the remnant capacity of each component before reaching the respective d_{ult}. For example, for a rockburst occurring upon cable bolt installation (d_0 = 50 mm), the d–E path ends at an ultimate displacement of 105 mm and an energy demand of 10 kJ/m^2 (see the light blue line in Fig. 10a). Accordingly, the d–E demand path exceeds the capacity of the cable bolts between 85 mm and the capacity of the Posimix bolts at 95–100 mm. The support system including the AS therefore collapses. For these specific loading conditions and the sequential failure of the two bolt types, the cumulative SSC further reduces from 30 kJ/m^2 to 24 kJ/m^2; the remnant capacity at cable activation is reduced from 23 kJ/m^2 to 17 kJ/m^2 (see Fig. 10b).

At the point of collapse, the theoretical remnant capacity is 13.6 kJ/m^2 (at red ' × '). However, the remnant capacity of the AS of 8.6 kJ/m^2 is no longer available due to the loss of support when the bolts fail. The available remnant capacity of (13.6–8.6 =) 5 kJ/m^2 is less than the energy demand (10 kJ/m^2). Some rock and support components are ejected at 100 mm of displacement. After subtracting the work done by the support from the energy demand, the energy available to eject rock is only 50% of the energy demand resulting from the rockburst. The installed support is therefore 50% effective, and the anticipated ejection velocity is less than that

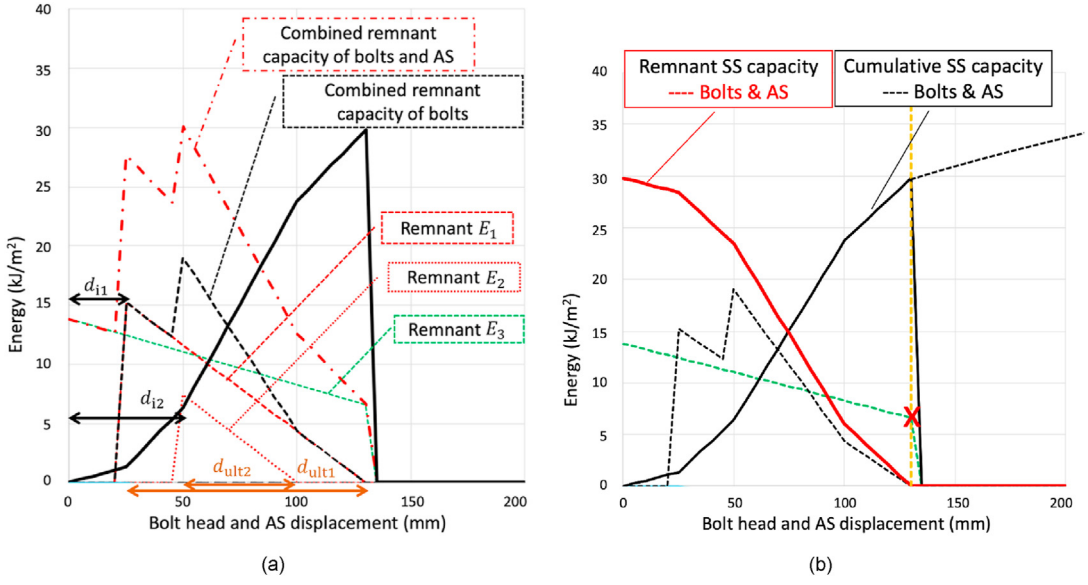

Fig. 9. Energy–displacement characteristics of the same support system as per Fig. 8 with a work split m = 25% for 25% indirect loading: (a) Remnant energy capacities of individual bolts, the AS, and the integrated/combined remnant support system; and (b) Same with cumulative mobilised SSC (black) and remnant SSC after support capacity consumption (red).

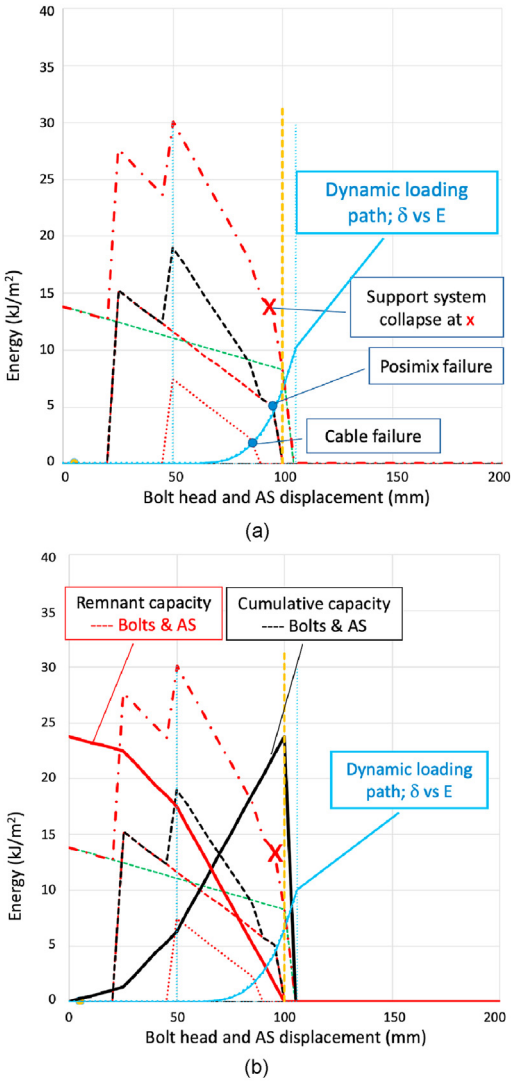

Fig. 10. (a) Energy–displacement characteristics of the same support system as per Fig. 9a, and (b) as Fig. 9b but loaded by a hyperbolic dynamic loading path from $E = 0$ kJ/m^2 at $d_0 = 50$ mm to $E = 10$ kJ/m^2 at $d = 105$ mm (curves without labels are introduced in Fig. 9a).

under unsupported conditions but not zero for the specified demands.

3.2.4. Implication for support design

The displacement capacity of a support system, when loaded by a rockburst, can be further compromised when support components fail sequentially (at 100 mm rather than 130 mm for the case in Section 3.2.3). Furthermore, the energy capacity can also be compromised because part of energy dissipation capacity of the AS is lost when the bolting system fails.

Not only can much of the support system's initial energy capacity be consumed by mining-induced deformations, but it may also not be available when needed if support components fail sequentially and lead to a premature collapse of the integrated support system. This example again underlines the need for DBSD. Without consideration of the displacement history, the available displacement and energy capacity will be overestimated.

In summary, the overall and local SSC models demonstrate that the SSC is highly influenced by the displacement history, i.e. the demand path the support experiences during the static and

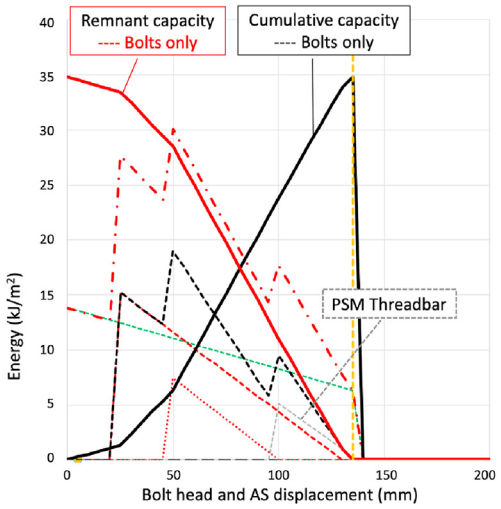

Fig. 11. Energy–displacement characteristics of a support system consisting of the support of Fig. 8 after PSM with 22 mm threadbar at 1.3 m spacing (installation sequence: Posimix bolts at 25 mm, cable bolts at 50 mm, and threadbar at 100 mm). Curves without labels are introduced in Fig. 9a.

dynamic loading process. The installation sequence affects the initial displacement or displacement at support activation and the mining-induced displacements after support installation consume part of the SSC. Furthermore, the displacements imposed during a rockburst reduce a support's energy capacity. These aspects are accounted for when following the DBSD principles.

Other factors that may affect the SSC can be assessed by more sophisticated versions of the above-presented capacity model but are beyond the scope of this article. Adjustments may have to be made, for example, for the impact of differential stress redistribution from failing bolts and increases in effective span of the AS upon failure of individual bolts, which reduces the capacity of the AS. Furthermore, adjustments for energy demand reducing effects by work done by bolts internal to the rock mass can be made and this may increase the overall and local support system capacities. The LSSC model is particularly relevant when strainburst occurs inside the reinforced rock mass and rock bolts are strained by the violent bulking of stress-fractured rock.

3.3. SSC consumption and restoration

Fig. 9b shows that energy capacity is consumed (red line) as the support system is deformed and the support is forced to do work. In other words, the remnant capacity is much lower than the 'installed' capacity because some of the 'installed' capacity has been consumed by mining-induced displacements.

This is of particular importance in burst-prone ground when energy demands are imposed on a deformed support system by a distant seismic event or a strainburst behind or inside the reinforced rock arch. This explains why support damage is often observed even though relatively small dynamic demands from distant seismic events are imposed on the support system. If the remnant capacity is low, the excavation becomes fragile, and minor rockbursts can inflict rather severe damage. For example, a relatively minor strainburst close to the excavation wall, i.e. inside the reinforced rock arch, can cause severe local support damage as previously discussed.

3.3.1. PSM

An underlying principle of the DBSD approach is that if support capacity can be consumed, it can also be restored by various means

of timely PSM. Proactive actions, e.g. by installing additional bolts after the support system has been deformed, can increase the ultimate load, displacement, and energy capacity (see Fig. 11 for energy capacity maintenance).

PSM using 22-mm diameter threadbars installed and activated at 100 mm of displacement, i.e. immediately after the cable bolts are anticipated to have reached their displacement capacity, increases the energy capacity (black line) by 17% from 30 kJ/m^2 to 35 kJ/m^2 (see Fig. 11). Immediately after PSM at 100 mm, the remnant energy capacity is 1.8 times higher (11 kJ/m^2 rather than 6 kJ/m^2). The threadbars, if long enough, can also restore the holding capacity of the failed cable bolts. This will offer an additional reserve against shakedown failure. In addition, the PSM bolts restrain further bulking and offer shear resistance that is frequently needed when a support system is severely deformed.

This PSM approach has been implemented and successfully operated since 2017 at a deep operating caving mine. At this operation, the preventive support maintenance is applied twice, first when the central displacement limits of 75 mm is reached (PSM1), and then when 125 mm is reached (PSM2). In some instances, a third PSM3 is installed at 175 mm if the integrity of the AS system has not been compromised.

3.3.2. *Implication for support design*

It is evident from the above examples that the available energy capacity of a support system is controlled by the previously imposed mining-induced displacements and the displacements imposed by a rockburst. The capacity of the support when needed is always (much) lower than the installed capacity. The anticipated displacement path therefore must be considered in support design, and the three interlinked design criteria for load, displacement, and energy capacities need to be simultaneously followed. Furthermore, proactive SSC restoration by PSM can offer cost-effective means for ground control (Moss and Kaiser, 2021).

3.4. *Practical implementation of deformation-based support design concepts*

In moderately to highly stressed ground, bulking mechanisms in hard rock, and dilation of yielding ground impose large displacements on the support, i.e. displacements that consume some of the capacity of the support system before it may be critically loaded, e.g. during a rockburst. Of the three demands, i.e. load, displacement, and energy, the displacement demand can be most readily observed in a qualitative or quantitative manner. Displacement records therefore serve as a means to calibrate and validate the DBSD approach. However, observation of measurable deformations is not a prerequisite for the application of DBSD principles. Even if little or no deformation of the support is observed during loading, displacements will still be imposed, particularly by bursting ground, during the rock mass failure process, and the support has to 'survive' the imposed deformations.

The DBSD approach is therefore also applicable for civil tunnelling, even when rather small and often unmeasurable displacements are encountered before a rockburst occurs, because large displacements are imposed on the support once excavation damage is caused by a strainburst. Whereas displacement monitoring cannot be used to assess the rockburst hazard (likelihood of occurrence), the DBSD approach is applicable when rockburst damage with both displacement and energy demands is anticipated. There is a basic difference between civil and mining applications in that the initial and pre-event displacements are typically smaller in civil tunnelling. Interestingly, the DBSD model shows that the LSSC may be lower in situations with little pre-event deformation.

In conditions of dynamic loading, energy emitted from a distant seismic source must also be dissipated. Given that the support pressure capacity of various support systems ranges in a rather narrow band (typically between 0.1 MPa and 1 MPa), the deformability is the most meaningful engineering design criteria. The displacement serves as a proxy of energy capacity consumption (that cannot be directly measured or qualitatively observed) because the product of support force times displacement represents the work done or energy dissipated by the support system.

Furthermore, it is a well-known engineering principle that stiff structures attract load while flexible structures shed load. Therefore, support systems must be deformable to prevent overloading when large displacements are anticipated. This deformability reduces the likelihood of support system damage.

Finally, if a large mass of reinforced rock is deformed or displaced, it dissipates energy and can sustain high energy demands. Deformability increases the ability of the reinforced ground to dissipate energy. By offering a large coherent mass of reinforced ground in the form of 'gabion panels', the detrimental effects of

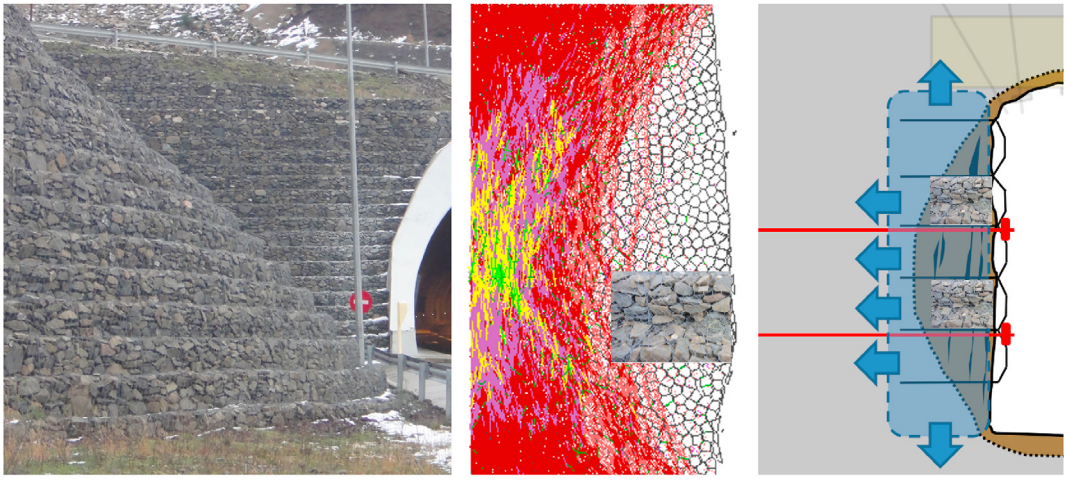

Fig. 12. (a) Gabion retaining wall (Photo courtesy M. Diederichs); (b) Deformed shape of Voronoi pillar model at 1% tangential strain with major principal stress vectors showing hour-glassing mode of failure (with image of stress fractured rock); and (c) Gabion support analogue for ground control in walls of drifts (modified after Kaiser, 2014).

energy or momentum transfer during dynamic loading by distant seismic events are lowered.

3.4.1. 'Gabion panel' concept

A gabion (from Latin 'cavea' meaning 'cage') is a cage filled with rocks for use in civil engineering, road building, and landscaping applications. A gabion wall is a retaining structure made of stacked stone-filled gabions tied together with steel mesh (see Fig. 12a). Internal to each gabion, bulking is restrained by the mesh resisting the desired movements of individual rock blocks. The gabion concept has been widely applied in slope retention and has been expanded via the reinforced earth concept.

By analogue, the 'gabion panel' support concept for ground control was developed by the lead author in 2012 to support stress-fractured ground (illustrated by the Voronoi model in Fig. 12b). As discussed above, this stress-fractured ground becomes prone to bulking during mining-induced straining. By creating stacked gabions of stress-fractured rock (Fig. 12c) to form a 'gabion panel' retained by mesh or shotcrete and tied together with rockbolts or cable bolts, the benefits of gabion retaining systems can be captured for the control of large mining-induced deformations. Such 'gabion panels' provide bulking control and reliable retention capacity inside the panel, add confinement to the ground behind, and enhance the tangential load bearing capacity to reduce roof sag and tangential straining of the walls. Furthermore, they retain broken rock (white zone in Fig. 12b) during confinement loss in unloading situations, e.g. at the extraction level of a caving operation.

In highly stressed brittle failing rock, spalled and fractured rock can form a skin of cohesionless, broken rock around excavations. If reinforced, the broken rock can become self-stabilising, as demonstrated by Lang (1961) for the Snowy Mountains Authority, Australia, and later by graduate students of the rock engineering program at the University of Toronto (see Fig. 13a–c, Hoek, 2007). The broken rock forms a 'panel' of stacked gabions, i.e. a 'gabion panel' (see Fig. 13d). This 'gabion panel' provides confinement (orange arrows) to the rock behind the panel and resists tangential (vertical) loads or displacements imposed on the panel. It also provides a coherent mass of supported ground. With a robust AS, such panels can retain their integrity while being rotated and translated as evidenced by the strainburst-damaged tunnel wall (see Fig. 13e).

The 'gabion panel' concept aims at creating deformable self-supporting rock panels in the walls by stacking gabions of broken rock.

3.4.2. Deformable arch concept

In civil tunnelling, yielding steel arches and longitudinal slots are used in weak ground to prevent excessive build-up of hoop stresses in shotcrete linings (Moss and Kaiser, 2021). In mining applications, stable deformable arches can be established in moderately deformed conditions without steel arches by stacking panels of reinforce rock, called 'stacked gabion panels'.

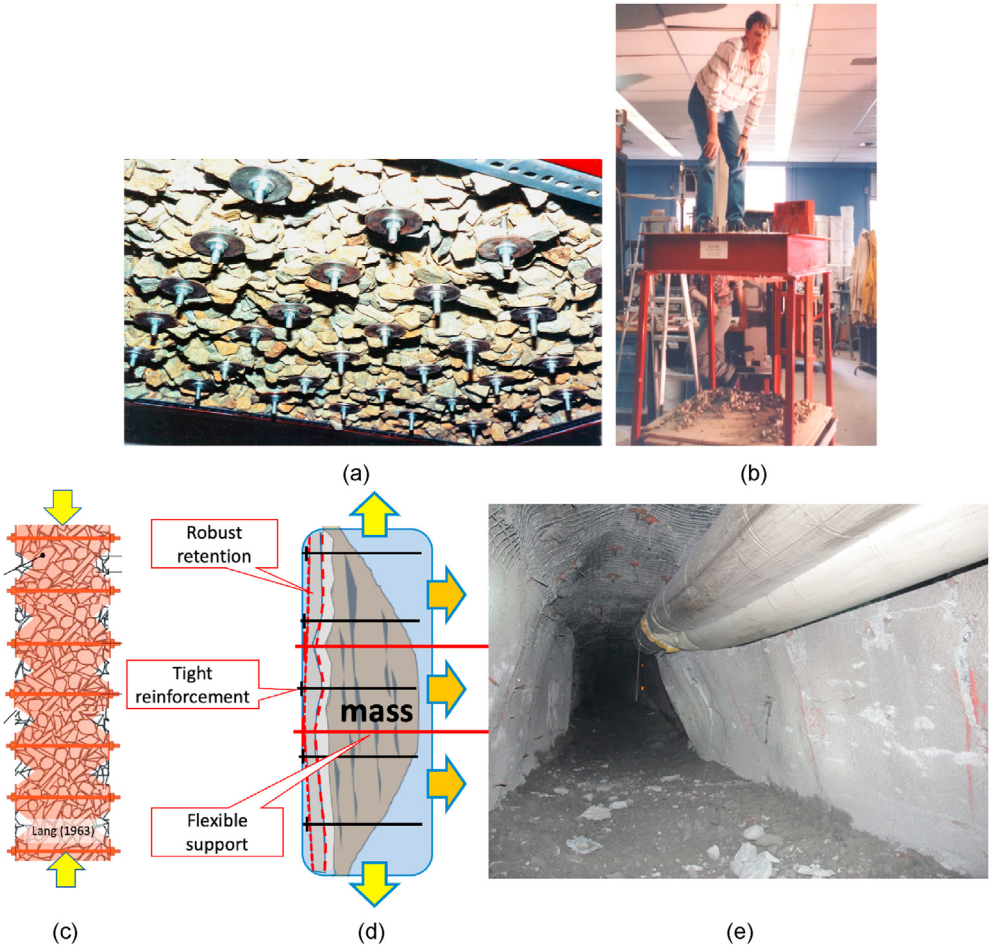

Fig. 13. Gabion panel concept: (a) Reinforced broken rock; (b) Capacity tested at University of Toronto (by Denis Shannon) in restraining steel frame (Hoek, 2007); (c) Rotated section through reinforced broken rock to serve as illustration of 'gabion panel' concept; (d) Critical elements of panels: retention, reinforcement, and tieback (yellow arrows represent tangential resistnce forces; orange arrows represnet lateral confinement pressures); and (e) Example of deformed but stable 'gabion panel' (courtesy: PTFI; Moss and Kaiser, 2021).

For pillar support in strainbursting ground, single wall panels provide the ductility required to accommodate large lateral bulking movements (see Fig. 13e).

The key characteristics of strong deformable support panels are highlighted in Fig. 13d. The 'gabion panels' have to:

(1) provide deformability both inside the 'gabion panel' and of the entire panel relative to the surrounding ground;
(2) provide tangential and lateral resistances while deforming into the excavation;
(3) be able to dissipate energy; and
(4) maintain substantial remnant load and energy capacities as the panels are deformed.

In summary, the DBSD approach aims at providing a sound engineering approach that accounts for the detrimental impact of mining-induced deformations on the support system and offers a safe and cost-effective solution that can be verified based on measurable entities, i.e. convergence and rock mass strain near the excavation. It extends the concept of self-supporting ground arches to conditions of statically and dynamically stressed ground.

4. Quantification of safety margins with DBSD approach

Once a support design has been quantified, it is necessary to verify whether the safety margin is sufficient for the anticipated use of the excavation, the ground conditions, and the anticipated demands. The factor of safety concept can be adapted to characterise the safety margin of a support system in a deterministic manner and for probabilistic design procedures by accounting for the variability in support demand and capacity. The deterministic approach is used here to demonstrate that the common definition of *FS* in terms of installed rather than remnant support capacities is flawed and typically leads to non-conservative support designs. In particular, it is demonstrated that energy-centric designs with FS_E defined by the ratio of the 'installed' energy capacity to the anticipated energy demand are deficient.

4.1. Remnant factor of safety

Because support capacity is consumed when deformed, it is essential to design for a remnant FS^r, defined as the ratio of the 'remnant SSC' to the 'critical demand' when the support is needed, i.e. for the most critical demand condition with the available, remnant SSC.

For the following three demand processes, the respective factors of safety for static or dynamic loading are written in Eqs. (2)–(4):

(1) Static and dynamic loading by structurally controlled 'wedges', and blocky or stress-fractured and unravelling ground;
(2) Displacements from static and dynamic elastic and inelastic deformations (e.g. bulking and bursting) near the wall or roof, and inside the reinforced rock mass; and
(3) Potential and kinetic energy release imposing energy demands on the AS and the reinforcement components by direct and indirect loading.

The respective factors of safety for static or dynamic loading are:

$$FS^r_L = \frac{SSC^r_L}{SD_L} \tag{2}$$

$$FS^r_D = \frac{SSC^r_D}{SD_D} \tag{3}$$

$$FS^r_E = \frac{SSC^r_E}{SD_E} \tag{4}$$

where *SS* represents the support system, SSC^r_L is the remnant load capacity of the *SS*, SD_L the load demand, SSC^r_D the remnant displacement capacity of the *SS*, SD_D the displacement demand, SSC^r_E the remnant work capacity of the *SS*, and SD_E the energy demand.

For relatively low stress environments and in good to poor ground, the design goal is to hold volumes of structurally controlled rock blocks or wedges in place or to make the rock mass self-supporting (Hoek, 2007) and to create stable rock arches (Lang, 1961) to prevent unravelling of blocky ground. In these situations, pre-failure displacements are small (mostly elastic) and cannot be used as instability indicators. The support design then focuses on static or dynamic force equilibrium to prevent falls of ground or shakedown failures. The safety margin is defined in terms of remnant load capacity and demand (FS^r_L).

For underground excavations in highly stressed and very poor quality ground, the design goal is to make the rock mass self-supporting while allowing it to yield and deform. In these situations, displacements are measurable and can be used as instability indicators. The support design is then focused on static or dynamic force equilibrium to prevent falls of ground or shakedown failures, on displacement compatibility with installed support components and support systems during rock mass yield, and on energy consumption during dynamic loading. Under static loading, the *FS* is defined in terms of load and displacement capacities and demands ($FS^r_{L,D}$). For dynamic loading, the safety margin should also be assessed in terms of energy capacities and demands (FS^r_E). For this purpose, the support system demand estimation procedures in Section 2.3 and the SSC estimation procedures in Section 3 are used.

Satisfying the required safety margin in terms of one of these three criteria is necessary but often not sufficient. The first two must be satisfied for static loading and all three for dynamic loading. Numerically, the three *FS*-values are not identical: generally, FS^r_E should be larger than FS^r_L and FS^r_D. Because of the complexities of energy transmission and the power law dependence of kinetic energy on the velocity, it is meaningful to set $FS^r_E = FS^2_L$ or FS^2_D, e.g. for $FS_L = FS_D = 1.5$, $FS_E = 2.25$.

The static *FSs* in terms of load $FS^r_{s,L}$ and displacement $FS^r_{s,D}$ are used to quantify the vulnerability of an excavation at a given stage in the design life. For the initial or installed $FS^{r,i}$, the installed capacity is used in the *FS* equations (see Eqs. (2)–(4)). It is only valid if no support capacity has been consumed by the mining-induced deformations since support installation.

As discussed above, some of the SSC is likely consumed before the system is critically loaded, and the demand changes with time due to mining-induced stress changes, deformations, or energy releases. This reduces the *FS* over the life of a support system. It is therefore meaningful to define FS^r as the ratio of remnant capacity to critical demand at the time when the support is needed. This is illustrated by Fig. 14 with three definitions of the safety margins (*SM*) indicated by green arrows.

For this example, the displacement demand is 50 mm after 20 mm of pre-event deformation (for a total of 70 mm) and the energy demand is 5 kJ/m^2. By conventional definition, i.e. comparing the demands to the installed capacities (at zero

displacement), $FS_E \geq 32/5 = 6.4$ and $FS_D = 135/50 = 2.7$. At the time of the rockburst, after 20 mm mining-induced displacement, $FS_E = 31/5 = 6.2$ and $FS_D = (135 - 20)/50 = 2.3$. However, after 70 mm of pre-event plus rockburst displacements, $FS^r_E = 18/5$ kJ/m^2 = 3.6 kJ/m^2 (vertical green arrow). In terms of displacements, at 5 kJ/m^2 energy demand, the displacement demand is 50 mm with a capacity of (115 − 20 =) 95 mm for a $FS^r_D = 1.9$. These remnant *FS*s are drastically lower than the initial installed *FS*s.

Furthermore, considering that the demand path (energy as function of displacement) is inclined during a rockburst (light blue), the most realistic safety margin is a function of energy and displacement demand ($SM_{D\&E}$). For the example shown in Fig. 14, the remnant capacity is reached along the loading path at 90 mm and 11.5 kJ/m^2. The conditional remnant *FS*s, when both displacements and energy increase to the point of failure, are obtained by relating to the point of failure at the end of the inclined green arrow ($SM_{D\&E}$). For an energy demand of 5 kJ/m^2 and a capacity of 11.5 kJ/m^2, $FS^r_E = 2.3$; and for a displacement demand of 50 mm with a capacity of (90 − 20 =) 70 mm, $FS^r_D = 1.4$. The conditional remnant *FS*s are lower than the *FS*s based on energy or displacement alone. Considering the elevated uncertainty when assessing energy demands and the suggested relation between the energy and displacement *FS*, $FS_E = FS^2_D$, the conditional *FS* ranges from 1.4 to 1.5 (i.e. sqrt(2.3)). In other words, this support will exhibit a marginal safety margin of $FS \leq 1.5$ when impacted by a rockburst with the defined energy and displacement demand after 20 mm of mining-induced deformation. For a second (equivalent) seismic event occurring after the first event (after 70 mm pre-event support deformation) the remnant factors of safety FS^r_E and FS^r_D will be less than 1.

Clearly designing rock support without consideration of the mining-induced deformations leads to false impression of safety. To establish a support system's *FS* against rockburst loading, it is necessary to simultaneously assess the *FS*s in terms of load, displacement, and energy. This reinforces the need for a deformation-based design approach.

Because of these complexities in establishing deformation-dependent *FS*s and the applicability limit of a support system, it is meaningful to reverse the *FS* equations (see Eqs. (2)–(4)) to define allowable load ($SD_{all,L}$), displacement ($SD_{all,D}$), and energy ($SD_{all,E}$) demand values:

$$SD_{all,L} = \frac{SSC^r_L}{FS^r_L} \tag{5}$$

$$SD_{all,D} = \frac{SSC^r_D}{FS^r_D} \tag{6}$$

$$SD_{all,E} = \frac{SSC^r_E}{FS^r_E} \tag{7}$$

It follows that the limits of a support system are best described in terms of allowable energy and displacement demands, or allowable ground motion (AGM) and displacement limits. In other words, the characteristic of a given support system and its limits of applicability are best described by AGM charts presenting the AGM as a function of the imposed displacement. The DBSD model was used to generate an illustrative example of an AGM chart.

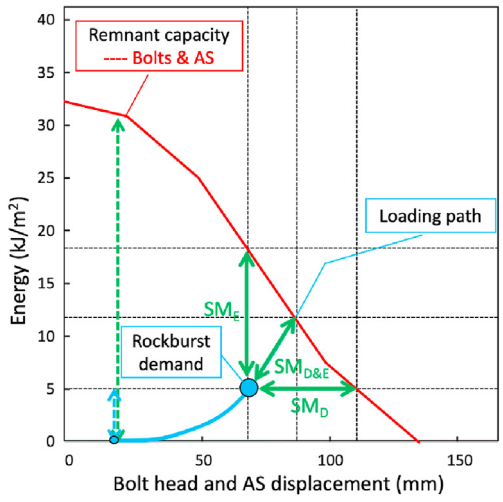

Fig. 14. Illustration of three *SM* definitions (green) indicating the proximity of remnant SSC (red) to the ultimate displacement and energy demand (blue circle) resulting from the rockburst loading path (blue). The *SM* equals the remnant SS capacity minus the respective seismic event demand in terms of energy or displacement or a combination thereof (D&E).

4.2. AGM charts

Conventionally, a support system is designed to survive a specified seismic event with a desired FS_E, e.g. an event with $M_L = 3.5$ at a distance $R = 30$ m or a design ground motion PGV^D. Because of the dependence of FS_E on displacements, this approach is not meaningful. It is more appropriate to define an AGM PGV_{all} (= PGV^D/FS_E) for a given support system and desired safety margin, and to use it to assess the acceptability for a given support design.

As previously described, the support capacity is reduced by imposed mining-induced bulking deformations and the displacements induced by the bulking of stress-fractured rock during a triggered or dynamically loaded strainburst. This means that the PGV_{all} decreases with increasing support displacement and drops to zero when the ultimate displacement capacity of the support system is exceeded. By using the DBSD approach, it is possible to establish the limitation of a support system in terms of the combined ground motion and displacement demands. An illustrative example is presented by the AGM chart in Fig. 15. It presents the AGM (PGV_{all}) as a function of *BF* (primary horizontal axis) and the total bolt head displacement (secondary horizontal axis) caused by stress-fractured ground during a dynamically loaded strainburst.

This chart illustrates that the allowable energy capacity defined by the AGM decreases with increasing bulking and with decreasing support energy efficiency (SEE; full and dotted black lines for 100% and 0% efficiency, respectively). The allowable limits for selected *FS*s can then be established (shown in green for *SEE* = 100% and 0% with $FS_E = 2.25$ and $FS_D = 1.5$, respectively). For simplicity, these limits can then be approximated as shown for *SEE* = 100% and 0% in full and dotted red lines, respectively. These thresholds characterise this support system and its limits of acceptability.

For this example, the desired *FS*s can be achieved if the ground motion hazard in terms of a design ground motion PDG^D/FS is no more than 2.2 m/s (for *SEE* = 100%), and the stress-fractured ground bulks by no more than 6%, or the total displacement is less than 90 mm. If the support system is less effective, the allowable limit may be reduced to $PDG^D/FS \leq 1.1$ m/s for an ineffective support with *SEE* = 0% with no more than 5% bulking or less than 80 mm total displacement. Every support system has its unique AGM chart.

4.3. Assessment of support systems with comparable AGM ratings

The DBSD model was applied to two support systems (SS1 and SS2) with different cumulative energy ratings: SS1 is rated for a nominal 20 kJ/m^2 with debonded bolts only, and SS2 for 31 kJ/m^2 with supplemental plain cables. When dynamic loading induces displacements by the bulking of stress-fractured rock, the imposed deformation can lead to local bolt or cable failures. In this case, the cable bolts in support system SS2 get overloaded first (see Fig. 10a) because they are less ductile than the debonded bolts and contribute little to the ductility/displacement capacity of the support system.

By adopting the DBSD model and the AGM chart approach, it can be concluded that the displacement and energy capacity of these two support systems are similar in terms of allowable *PGV* and bulking limits (results not shown) despite the fact that SS2 has a 50% higher nominal energy capacity. This must not be misinterpreted as meaning that the two support systems are equivalent when considering other relevant design criteria. Whereas the two support systems are essentially equal from an energy and displacement capacity perspective, they are not when considering three other support functions:

(1) Load capacity (e.g. for back and intersection support): SS2 has 2.5 times higher load capacity than SS1.
(2) Retention capacity of the AS: an otherwise equivalent AS has a much higher capacity when used with SS2 due to the much shorter effective span with twice as many bolts. The static load from stress-fractured rock is more than 2 times higher for SS1 due to wider effective spacing and the dynamic energy impact is approximately 4 times higher for SS1. Consequently, the retention capacity of the SS2 is 4 times higher than that of SS1.
(3) Bulking control to reduce the displacement demand during a strainburst: with almost 2 times more bolts per cubic meter, bulking and strain localization are more suppressed within the first 2–3 m from the excavation wall with SS2. This can drastically reduce the displacement demand and thus lead to a superior performance of the SS2.

Consequently, SS2 is more robust than SS1, not because of higher energy or displacement capacities but because of higher load and retention capacities, and hence a better ability to control bulking. The value of the more expensive SS2 is in increasing the safety margin of the backs of the excavations by ensuring reliable retention of broken rock, load transfer to bolts, and reducing displacement demands on both the AS and the rock reinforcement. Neither the energy-centric nor the deformation-based design approach account for these often-dominant design criteria.

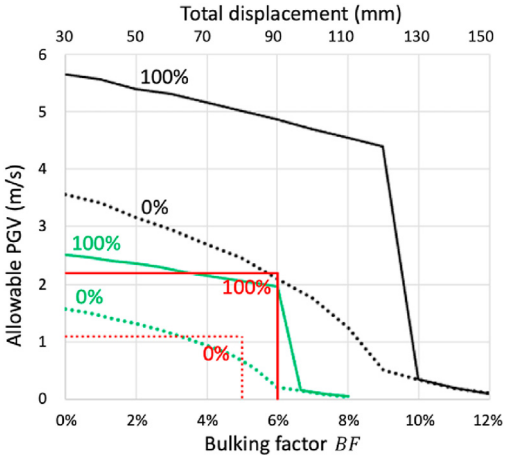

Fig. 15. Illustrative example of an AGM chart for a given support system (with debonded Posimix and cable bolts at 0% and 100% efficiency) and a rockburst anticipated after 30 mm of pre-event displacement.

5. Conclusions

The primary objective of this article is to introduce the DBSD approach for static and dynamic conditions and to apply it to typical hard rock ground conditions in deep mining operations.

For the selection of efficient and effective rock support systems, it is important to first assess the vulnerability of an excavation to static and dynamic disturbances. This article provides the behavioural background for support system selection, particularly for the support of brittle failing ground. Simple means for estimating displacements caused by mining-induced stress changes are provided to illustrate the application of the DBSD approach. It complements existing support design approaches.

As support is deformed, individual support components get simultaneously deformed and some of the support's capacity is consumed, i.e. the remnant capacity decreases gradually to zero when the integrated support system fails. The support consumption evolution therefore must be accounted for when designing support for mining and rockburst applications.

If the SSC can be consumed, it can also be restored by PSM. In many mining situations, it may be more cost-effective to let the support deform before installing less ductile high-capacity support components.

The remnant factor of safety concept with FS^r = *remnant capacity*/*critical demand* is adopted to characterise the safety margin of support systems. In mining, FS^r changes with time. The capacity and the demand may change due to mining-induced stress changes, imposed deformations or various forms of energy release. For this reason, it is most meaningful to design for a remnant FS^r at the time when the support is needed, i.e. under the most critical demand condition with the then available or remnant SSC.

A sufficiently high *FS* when the support is needed, e.g. during a rockburst, is a necessary but not necessarily sufficient design criterion. Two support systems may be essentially equal from an energy and displacement capacity perspective. However, they may differ when considering the robustness of a support system. The ability of a robust support system to withstand adverse conditions is often controlled by the holding and retention functions of the support system. For this reason, support systems with deep holding elements (cable bolts) and denser bolting patterns are proven to be more robust.

Robust support systems also positively alter the displacement and energy demands and the self-supporting capacity of the rock mass. This often improves a support system's performance for reasons other than their energy and displacement capacities.

From a comparison of two support systems with similar energy and displacement capacities, it is concluded that:

(1) Energy- and deformation-based design considerations are necessary but not sufficient criteria in support design. Load, retention, and bulking control criteria should also be met.
(2) The rock mass must be effectively reinforced to control and minimise bulking near the excavation wall.
(3) Much of the theoretically available (nominal) support capacity may be consumed when needed. The AGM at the time of a seismic event may be lower or zero due to mining-induced support deformation. Therefore support should be designed for a specified strainburst, remote

energy demand (*PGV*), and an anticipated pre-event deformation.

The motivation for the proposed changes in design methodology is in part driven by technology developments that allow to rapidly and reliably measure the excavation and support responses to mining in terms of displacements. Major advances in open pit design have been made in recent years by integrating radar-based slope movement monitoring into the design process. By analogue, by following the DBSD principles, design models can now be calibrated and verified, and operational decisions can be based on real-time observations. The safety margin of a gradually deformed support system can be assessed, and PSM can be targeted and executed in a cost-effective manner.

This article provides means to move toward 'best practices in support design' by developing support design principles and standards for safe and cost-efficient ground control, and by achieving consistency across operations. Although there is ample qualitative evidence supporting the findings presented here, site-specific verification and iterative modifications will be required to apply these concepts without undue risk. It is of paramount importance that the results from DBSD are carefully verified and, if necessary, modified based on systematic deformation and support performance monitoring.

Finally, the merit of the approach outlined in this article is that it demonstrates that current support selection and design practices are missing one key factor, i.e. that consumption of displacement capacity reduces the effectiveness of a support system which must be accounted for.

Declaration of competing interest

The authors declare that they have no known competing financial interests or personal relationships that could have appeared to influence the work reported in this paper.

Acknowledgments

The efforts of many individuals and their supporting companies including PT Freeport Indonesia (PTFI) and Newcrest deserve to be thankfully acknowledged. The list is too long to name all contributors, but we wish to especially thank Matt Sullivan (PTFI), Jared De Ross (Newcrest) and Ming Cai (Laurentian University) for their contributions. This work would not have been possible without the financial support of NSERC (Canada's Natural Sciences and Engineering Research Council), and ORF (Ontario Research Fund), as part of the SUMIT (Smart Underground Monitoring and Integrated Technologies for deep mining) program at the Centre of Excellence for Mining Innovation (CEMI).

List of acronyms

d_{ult}, δ_{ult}	Ultimate displacement capacity of bolts and areal support
F_m	Mean force representing the actual load displacement curve of support components
FS	Factor of safety; superscript 'r' for remnant
PGV	Peak ground velocity; subscript 'all' for allowable, superscript 'D' for design
SC	Support capacity (subscripts L, D, and E for load, displacement, and energy, respectively)
SD	Support demand (subscripts L, D, and E for load, displacement, and energy, respectively)

Appendix A. Supplementary data

Supplementary data to this article can be found online at https://doi.org/10.1016/j.jrmge.2021.05.007.

References

Cai, M., Kaiser, P.K., 2018. Rockburst phenomena and support characteristics. In: Rockburst Support Reference Book, I. Laurentian University, p. 191.
Dick, G., Nunoo, S., Smith, S., Newcomen, W., Kinakin, D., Stilwell, I., Danielson, J., 2020. Monitoring and managing large deformation pit slope instabilities at a British Columbia copper mine. In: Proceedings of the International Symposium on Slope Stability in Open Pit Mining and Civil Engineering. ACG, pp. 439–452.
Gao, F.Q., Kaiser, P.K., Stead, D., Eberhardt, E., Elmo, D., 2019a. Strainburst phenomena and numerical simulation of self-initiated brittle rock failure. Int. J. Rock Mech. Min. Sci. 116, 52–63.
Gao, F.Q., Kaiser, P.K., Stead, D., Eberhardt, E., Elmo, D., 2019b. Numerical simulation of strainbursts using a novel distinct element method. Comput. Geotech. 106, 117–127.
Heal, D., Potvin, Y., Hudyma, M., 2006. Evaluating rockburst damage potential in underground mining. In: Golden Rocks 2006 – Proceedings of the 41st U.S. Symposium on Rock Mechanics (USRMS). Paper Number ARMA-06-1020.
Hoek, E., 2007. Practical Rock Engineering. Hoek's Corner at Rocscience.Com, p. 341. https://www.rocscience.com/assets/resources/learning/hoek/Practical-Rock-Engineering-Full-Text.pdf (Accessed 6 July 2021).
Kaiser, P.K., McCreath, D.R., Tannant, D.D., 1996. Rockburst Support. MIRARCO - Geomechanics Research Centre. Laurentian University, Sudbury, Canada, p. 314.
Kaiser, P.K., Diederichs, M.S., Martin, C.D., Sharp, J., Steiner, W., 2000. Underground works in hard rock tunneling and mining. In: Proceedings of the GeoEng2000. Technomic Publishing Co. Inc., Lancaster, PA, USA, pp. 841–926.
Kaiser, P.K., 2014. Deformation-based support selection for tunnels in strainburst-prone ground. In: Hudyma, M., Potvin, Y. (Eds.), Proceedings of the Seventh International Conference on Deep and High Stress Mining. Australian Centre for Geomechanics, Perth, pp. 227–240.
Kaiser, P.K., 2016. Ground support for constructability of deep underground excavations—challenge of managing highly stressed brittle rock in civil and mining projects. In: Proceedings of the ITA Sir Muir Wood Lecture of International Tunneling Association at World Tunneling Congress, p. 33.
Kaiser, P.K., 2017a. Chapter 15—excavation vulnerability and selection of effective rock support to mitigate rockburst damage. In: Feng, X.-T. (Ed.), Rockburst: Mechanisms, Monitoring, Warning, and Mitigation. Elsevier, New York, NY, USA, pp. 473–518.
Kaiser, P.K., 2017b. Ground control in strainbursting ground - a critical review and path forward on design principles. In: Proceedings of the 9th International Symposium on Rockbursts and Seismicity in Mines, pp. 146–158. Santiago, Chile.
Kaiser, P.K., 2019. From common to best practices in underground rock engineering. In: Proceedings of the Mueller Lecture, 14th ISRM Congress. CRC Press, pp. 141–182.
Lang, T.A., 1961. Theory and practice of rock bolting. Trans. Amer. Inst. Min. Engrs. 220, 333–348.
Morissette, P., Hadjigeorgiou, J., Thibodeau, D., Potvin, Y., 2012. Validating a support performance database based on passive monitoring data. In: Proceedings of the 6th International Seminar on Deep and High Stress Mining, pp. 41–55.
Moss, A., Kaiser, P.K., 2021. An operational approach to ground control in deep mines. J. Rock Mech. Geotech. Eng. https://doi.org/10.1016/j.jrmge.2021.05.008.
Potvin, Y., Hadjigeorgiou, J., 2020. Ground Support for Underground Mines. Australian Centre for Geomechanics, Perth, Australia, p. 520.
Stacey, T.R., 2016. Addressing the consequences of dynamic rock failure in underground excavations. Rock Mech. Rock Eng. 49, 4091–4101.
Terzaghi, K., 1946. Rock defects and loads on tunnel support. In: Proctor, R.V., White, T.L. (Eds.), Introduction to Rock Tunnelling with Steel Supports. Commercial Sheering & Stamping Co., Youngstown, OH, USA, p. 271.

Dr. Peter Kaiser is Professor Emeritus at the Laurentian University, and President of the GeoK Inc., Sudbury, Canada. He is a graduate of the Federal Institute of Technology in Zurich and the University of Alberta, Canada. He was Chair for Rock Engineering and Ground Control at Laurentian University in Canada and President of MIRARCO, a mining research centre he founded in 1997. Between 2007 and 2015, he was seconded to the Centre for Excellence in Mining Innovation (CEMI) as Founding Director and then as Director of the Rio Tinto Centre for Underground Mine Construction. He is a specialist in applied research for underground mining and construction and brings extensive experience from the industrial and academic sectors. He has supported contractors, mining companies and public sector clients in claims and litigations on four continents. He is the author of more than 400 technical and scientific publications and is a Fellow of the Engineering Institute of Canada and the Canadian Academy of Engineers. He was awarded the J.C. Smith Medal for "Achievements in the Development of Canada" and selected to present the Sir Allan Muir Wood lecture at the World Tunnelling Congress 2016 on "Challenges of tunnel constructability", and the Müller lecture at the ISRM Congress 2019 entitled "From common to best practices in underground rock engineering".